

This work was written as part of one of the author's official duties as an Employee of the United States Government and is therefore a work of the United States Government. In accordance with 17 U.S.C. 105, no copyright protection is available for such works under U.S. Law.

Public Domain Mark 1.0

<https://creativecommons.org/publicdomain/mark/1.0/>


Access to this work was provided by the University of Maryland, Baltimore County (UMBC) ScholarWorks@UMBC digital repository on the Maryland Shared Open Access (MD-SOAR) platform.

Please provide feedback

Please support the ScholarWorks@UMBC repository by emailing scholarworks-group@umbc.edu and telling us what having access to this work means to you and why it's important to you. Thank you.

Engineering Notes

Improving the VERITAS Orbit Reconstruction Using Radar Tie Points

Gael Cascioli*

University of Maryland, Baltimore County, Baltimore,
Greenbelt, Maryland 21250

Daniele Durante†

Sapienza University of Rome, Rome 00184, Italy

Erwan Mazarico‡

NASA Goddard Space Flight Center, Greenbelt, Maryland
21250

and

Mark Wallace,§ Scott Hensley,|| and Suzanne Smrekar¶
California Institute of Technology, Pasadena, California
91109

<https://doi.org/10.2514/1.A35499>

Nomenclature

N_{lm} = number of landmarks observed per orbit
 T = orbital period, h
 α = Earth angle

Subscript

lm = landmark

I. Introduction

THE recently selected NASA Discovery mission, Venus Emissivity, Radio Science, InSAR, Topography, and Spectroscopy (VERITAS), will orbit Earth's neighboring planet and gather foundational datasets that will address many open questions on its dynamic history and active geophysical processes [1]. The scientific objectives of VERITAS will be enabled by a gravity investigation, relying on the Integrated Deep Space Transponder (IDST) operating in both X- and Ka-band [2–4], the X-band Venus Interferometric Synthetic Aperture Radar (VISAR) [5], and an infrared spectrometer, the Venus Emissivity Mapper (VEM) [6].

To successfully acquire the high-accuracy scientific observations of VISAR and VEM, a precise knowledge of the probe's trajectory is required. Both these instruments produce georeferenced datasets, and thus the quality of the orbit prediction and the accuracy of the orbit

reconstruction play a key role in successfully planning the observations and precisely georeferencing the collected data, respectively. The processing of radar echo signals requires precise knowledge of the spacecraft trajectory, particularly for geological mapping purposes where 30-m-resolution radar images are combined into mosaics. Moreover, to substantially reduce downlinked data volume, synthetic aperture radar (SAR) image formation is done on the spacecraft, requiring trajectory knowledge onboard as well as after data collection for additional processing on the ground. The onboard preprocessing consists of the formation of interferograms (interference of multiple images of the same surface area) and multilook imagery (stacking of multiple images of the same surface area). Both these tasks require the knowledge of the acquisition geometry in terms of both attitude and position of the spacecraft. Relative errors between subsequent orbits can introduce discontinuities in the final products; thus the quality of orbit reconstruction and prediction plays a critical role not only for navigation operations but also for science return. In the early phases of the mission, the trajectory reconstruction operations will not benefit from the entire VERITAS dataset obtained at the end of the mission. Indeed, the day-to-day reconstructed orbits will invariably be more uncertain than the output of the final reprocessing, which will benefit from the much-improved determination of the Venus gravity field [3] and rotational state [2]. This indeed directly affects all the immediate science products and thus the observation planning operations. Specific data acquisition campaigns such as radar repeat-pass interferometry (RPI) require highly precise orbit reconstruction of the initial overflight and dedicated targeting of the “tube” entrance (see Table 2 in [7]). That reconstruction requires enhancing the standard Earth tracking-based orbit determination (OD), which employs range-rate (Doppler) data collected in the context of the gravity field investigation and for on-board ephemeris generation, with VISAR data. We report on the improvement in the preliminary OD performance attainable by VERITAS when combining Earth tracking data with repeated surface landmark observations (*tie points*) produced from the SAR data in greater detail than in previous work. Although in this work we focus on the tie point analysis for VERITAS, the presented method is general and could, in principle, be applied to any orbital mission with similar radar instrumentation and observation geometry. The capability of tie points to deliver improved orbital reconstruction and prediction performances analyzed and discussed in this work, coupled with the strong geodetic constraints they were shown to be (e.g., [2]), broadens their field of application not only for scientific research but also for operational scenarios.

In Sec. II we present the concept of tie points and discuss their use in the OD process; in Sec. III we discuss the numerical simulations we performed for assessing the accuracy of VERITAS orbit reconstruction and prediction, while in Sec. IV we present and discuss the results. Section V gives concluding remarks.

II. Radar Tie Points

VISAR will be able to penetrate the dense cloud layer of Venus, identify characteristic surface features, and measure their range and range-rate with respect to VERITAS, with an expected accuracy of 3 m and ~350 mm/s (or 10 Hz at X-band), respectively (see Appendix A.1 in [2] for additional details about the noise estimation algorithm). The VERITAS Science Phase II orbit is near-polar ($i \sim 85.4^\circ$), near-circular, low altitude (180×255 km), and near-frozen. The ground track repeats every 244 days. This is slightly longer than the 243-day Venus sidereal rotation period, and it is due to the very slow ascending node precession. The nominal mission consists of four such mapping cycles (or simply “cycles”) spanning 2.7 Earth years. After an orbital period of $T \sim 1.5$ h, the ground track

Received 27 June 2022; revision received 3 October 2022; accepted for publication 5 October 2022; published online 28 November 2022. Copyright © 2022 by the American Institute of Aeronautics and Astronautics, Inc. All rights reserved. All requests for copying and permission to reprint should be submitted to CCC at www.copyright.com; employ the eISSN 1533-6794 to initiate your request. See also AIAA Rights and Permissions www.aiaa.org/randp.

*Postdoctoral Research Fellow, Center for Space Sciences and Technology; also Planetary Geology, Geophysics & Geochemistry Laboratory, NASA Goddard Space Flight Center, Maryland 21250 and Center for Research and Exploration in Space Science and Technology, NASA/Goddard Space Flight Center (GSFC), Greenbelt, Maryland 20771.

†Assistant Professor, Department of Mechanical and Aerospace Engineering.

‡Research Scientist, Planetary Geology, Geophysics & Geochemistry Laboratory.

§Mission Analyst, Jet Propulsion Laboratory.

||Senior Research Scientist, Jet Propulsion Laboratory.

is shifted eastward by approximately 10 km at the equator, due to Venus's slow, retrograde rotation. This orbital configuration allows mapping the same surface feature both with a significant temporal difference (multiples of a half-period; four times ascending and four times descending, so eight times during the full mission), which we call *global tie points*, and between adjacent orbits (exploiting the 14.4 km swath width of the radar footprint), which we call *local tie points*. In previous works, the global tie points have been shown to be extremely helpful for complementing the ground-based radio tracking dataset for the determination of the rotational state and interior structure of Venus [2,8,9]. Instead, here we focus on the use of local tie points and show their benefits for reconstructing the VERITAS trajectory. Due to their nature, local tie points, once included in the navigation dataset, can impose constraints between adjacent orbits and, thus, in principle, enhance the observation geometry and lead to improved orbit reconstruction performance. Moreover, the landmark observations being relative to Venus, as opposed to the Doppler tracking measurements that are relative to Earth, the two datasets can provide complementary information able to strongly strengthen the spacecraft ephemeris solution. Chodas et al. [10] applied this data analysis strategy to NASA's Magellan, showing a significant improvement of the orbit reconstruction capability (the analysis was limited to a small number of orbits). It has been shown in Ref. [9] that in the case of Magellan the combined data analysis strategy reduced orbital errors by nearly an order of magnitude. The relative quality of the two datasets (Doppler and radar tie points) plays an important role, and thus the previously obtained Magellan results cannot be directly extrapolated to VERITAS as both the Doppler tracking system and onboard radar are profoundly different.

The tie point measurements are conceptually similar to altimetric crossovers (e.g., [11,12]). The two methods exploit overlaps of the instrument surface swaths (or footprints and profiles) to form repeated measurements. It is, however, worth underlining that, in addition to the relative radial distance between the spacecraft platform and the surface landmark, tie points can also provide constraints on relative velocity (Doppler).

The nominal tracking schedule foreseen for VERITAS assumes 8 h of tracking (~5 orbits) followed by 16 h of VISAR observations (~11 orbits), each day. This constitutes indeed another valid reason for augmenting the navigation solution, with a radar dataset that covers temporal gaps between ground contacts. Indeed, OD performance is

maximized when the spacecraft is being tracked and gradually degrades outside the tracking windows. Figure 1 shows a schematic illustration of the acquisition geometry of local tie points.

The radar observes Venus's surface with an off-nadir look angle of 30 deg (i.e., the radar boresight is inclined with respect to the nadir direction). The surface features used for tie point generation will be recognized using an automated scene matching algorithm [5]. The expected accuracy of ranging and Doppler tie point measurements, 3 m and 10 Hz, respectively, accounts for the spatially variable nature of the matching accuracy by adopting the average pixel accuracy retrieved from Magellan stereo data, corresponding to 0.2 pixel. During the 11 out of 16 total daily orbits, in which the radar observations will be collected, VISAR will continuously map the surface, providing complete global coverage of the planet over the whole mission.

In the following, we simulate three different cases assuming 10, 20, and 40 observed landmarks per orbit, corresponding to an average separation on the surface of 3800, 1900, and 950 km, respectively. To generate a random set of tie points in latitude and longitude avoiding spatial aliasing issues, we simulate twice the number of desired observed landmarks (N_{lm}) with uniform spacing in time ($\Delta t = T/2N_{lm}$, where T is the orbital period), with a 10% random variability on Δt , and then randomly subsample the $2N_{lm}$ generated landmarks down to the desired number.

III. Numerical Simulations

The OD process consists of the estimation of the spacecraft's dynamic model parameters that best fit the tracking data. Defining \mathbf{x}_0 as the dynamic model's state vector at a given time, the scope of OD is to find the value of \mathbf{x}_0 that produces an estimated trajectory as close as possible to the true trajectory. Due to the highly nonlinear nature of the OD problem, we employ the commonly used linearized formulation. All the quantities that appear in the following are to be intended as *deviations* (i.e., differences) with respect to a reference solution (e.g., $\mathbf{x}_0 = \mathbf{X}_0 - \mathbf{X}_0^*$, where the star denotes the reference solution).

The minimum variance least-squares estimate of the state vector, $\hat{\mathbf{x}}_0$, is (for the problem definition with a consistent nomenclature see, e.g., [13], or [14] Sec. III and references therein)

$$\hat{\mathbf{x}}_0 = (H^T R^{-1} H + \bar{P}_0^{-1})^{-1} (H^T R^{-1} \mathbf{y} + \bar{P}_0^{-1} \bar{\mathbf{x}}_0)$$

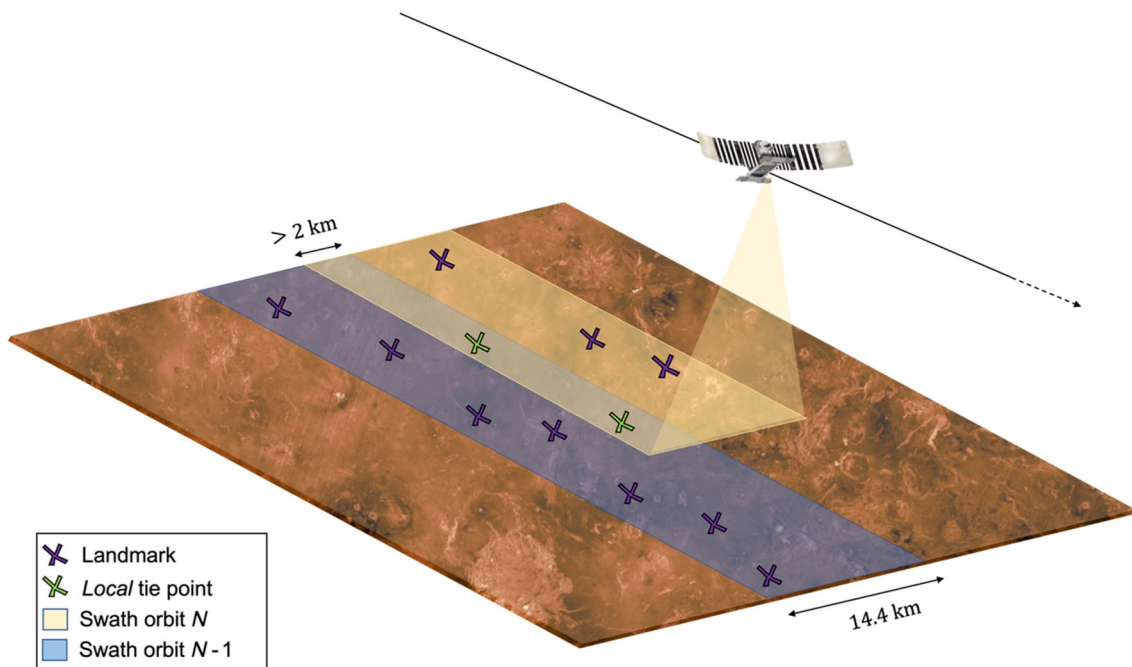


Fig. 1 Tie point acquisition geometry.

where H is the mapping matrix containing the partial derivatives of the observations with respect to the state vector components at the reference time, R is the observation noise covariance matrix (usually assumed to be diagonal), \bar{P}_0 is the a priori covariance matrix of the state vector components, y is the observation residuals vector, and \bar{x}_0 is the deviation of the a priori value of the state vector components with respect to iteration values.

The covariance matrix associated with the state vector is $P_0 = (H^T R^{-1} H + \bar{P}_0^{-1})^{-1}$. In this work, we are interested in assessing the time evolution of the accuracy of orbit reconstruction over one OD arc and thus in the time evolution of $P(t)$. The covariance matrix can be mapped linearly in time as

$$P(t) = \Phi(t, t_0) P_0 \Phi^T(t, t_0)$$

where $\Phi(t, t_0)$ is the state transition matrix, i.e., the quantity that maps the state vector between times t_i and t_j :

$$x_k = \Phi(t_k, t_j) x_j$$

In this work, we assume two-day data arcs (in line with navigation assumptions [7]) during which two 8 h two-way Ka-band Doppler tracking data batches are processed. The spacecraft tracking system, allowing simultaneous two-way X- and Ka-band Doppler and ranging, has heritage from ESA's BepiColombo mission and is expected to provide the same level of performance [1,2,4]. For Doppler data, we use a 10 s integration time and draw the Doppler noise from a uniform distribution ranging between 0.015 and 0.038 mm/s to account for the noise variability observed by Ref. [15], caused mainly by variable weather conditions at the ground station. For the tie point measurements we assume a noise level of 3 m and 10 Hz for ranging and Doppler, respectively (see Sec. II), and we assume a diagonal observation noise covariance matrix, corresponding to the hypothesis of independent observations. The dynamic model of VERITAS accounts for the gravitational attraction of Venus, both the static field (using the 180 deg and order MGNU180P gravity field determined by Magellan [16]) and its dynamic component (i.e., gravitational tides), the nonconservative accelerations due to solar radiation pressure, and atmospheric drag (using the VenusGRAM atmospheric model [17]). Using this dynamic model, we generate synthetic observables representing the navigation tracking *observables*, superimpose additive white Gaussian noise in line with the aforementioned assumptions, and use them in the OD filter.

The inclusion of radar tie points in the OD process is straightforward. Due to their nature, each individual radar observation can be treated as a couple of standard ranging and Doppler observations (if we were to make an analogy with Earth-based observations the spacecraft here acts as the ground station and the landmark acts as the

spacecraft). The observation equations and partial derivatives for ranging and Doppler are very well known (e.g., [18]) and can be easily implemented in the software. The formation of a "tie point" observation is obtained through the estimation of the physical location of individual surface features, which are observed multiple times. This allows the single observations to be referred to the same point on the surface of the planet and thus tied together.

The aim of this work is to assess the *initial* orbit reconstruction capability, i.e., when the tracking data are initially collected. This approach implies that we cannot leverage the full dataset of the VERITAS mission to constrain the Venus gravity field to the very high accuracy obtainable at the end of the mission [3]. Indeed, we assume that the relevant physical parameters appearing in the dynamic model of the OD filter are known to the level of the current, pre-VERITAS state-of-the-art (see Table 1).

In the OD estimation filter, we solve, at each arc, for the state of the spacecraft (position and velocity at reference time), Venus's sidereal spin rate to account for its recently reported potential variability ([19], as described in Ref. [2] Appendix A.2), spin pole initial direction and rate over the plane of the sky, the landmark positions (latitude, longitude, elevation), the mass of Venus, the static gravity field of Venus up to degree and order 15 (in accordance with the navigation assumptions [7]), the tidal Love number k_2 , and a scale factor for the solar radiation pressure acceleration. We do also estimate an impulsive change in velocity, ∇v , possibly associated to daily spacecraft momentum wheel desaturation maneuvers, and empirical along-velocity accelerations aiming at absorbing remaining mismodeled effects (e.g., atmospheric density variability). We model these accelerations as a stochastic white noise uncorrelated process. Although we may have an indication on the accuracy of the dynamic model (i.e., the a priori magnitude to be selected for empirical accelerations), assessing the temporal variability is more complex. This is generally done according to experience gathered once the spacecraft is flying. As a comparison, the baseline approach for analyzing Cassini tracking data was to use stochastic acceleration with an 8 h batch time [20]. However, they increased the update frequency when large maneuvers were performed or the spacecraft was close to Saturn periapsis. For VERITAS, the larger source of uncertainty is expected to come from variability of atmospheric density. Thus, we opted for analyzing two different cases for the update rate of empirical accelerations, 8 and 2 h, to assess the effect of different empirical parameterizations on the filter solution.

IV. Results and Discussion

Our simulations consist of a covariance analysis, using the NASA/JPL software MONTE [21], of 46 OD arcs representative of the entire span of possible viewing geometries from Earth. The first aspect to assess is the effectiveness of the inclusion of tie points in the orbit reconstruction of the probe. We adopt the case with 10 landmarks per

Table 1 A priori uncertainties used in the orbit determination filter

Parameter	A priori uncertainty	Source	Notes
VERITAS position (3D)	1 km	— —	Conservative assumption, not constraining
VERITAS velocity (3D)	1 m/s	— —	Conservative assumption, not constraining
Venus GM	$6 \times 10^{-3} \text{ km}^3/\text{s}^2$	[16]	Up to degree and order 15, in accordance with navigation assumptions [7]
Venus gravity field	As in MGNU180P	[16]	
Venus Love number, k_2	0.066	[25]	
Solar pressure scale factor	25%		Pessimistic assumption
Wheel desaturation maneuver (3D)	0.5 mm/s	[7]	Corresponding to the 61 ppm maximum observed variation
Sidereal spin rate	$1.4 \times 10^{-11} \text{ rad/s}$	[19]	
Pole right ascension	2.8 arcsec	[19]	
Pole right ascension rate	0.34 deg/century	Derived from [19]	Using Eq. (A6.30) from Ref. [2]
Pole declination	2.5 arcsec	[19]	Using Eq. (A6.30) from Ref. [2]
Pole declination rate	0.20 deg/century	[19]	
Empirical accelerations	$6.0 \times 10^{-11} \text{ km/s}^2$	[7]	
Landmarks radial positions	1.0 km	— —	Conservative assumption, not constraining
Landmarks latitudinal position	6.0 km	— —	Conservative assumption, not constraining
Landmarks longitudinal position	6.0 km	— —	Conservative assumption, not constraining

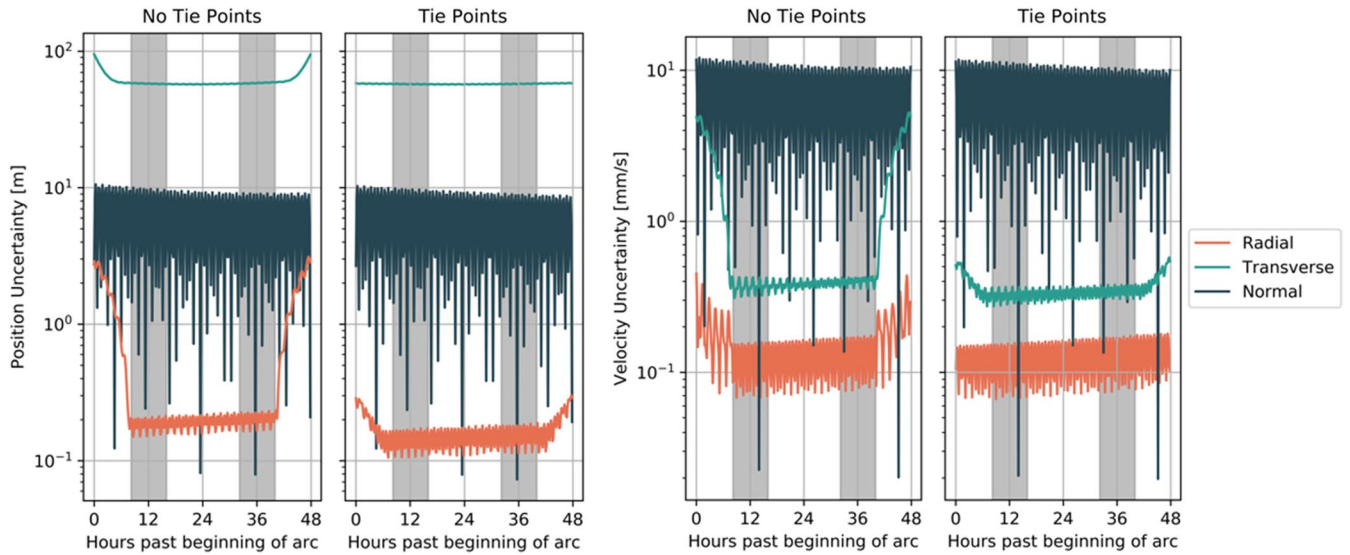


Fig. 2 Position and velocity uncertainty during an OD arc with and without the inclusion of tie points (10 per orbit).

orbit as baseline, and then comment on the improvements brought by augmenting the number of included tie point observations. Figure 2 reports the position and velocity uncertainties, in terms of their radial, transverse, normal (RTN) direction components over one OD arc in the baseline case.

The tie point improvement on the trajectory reconstruction is clearly noticeable with a general decrease of the position and velocity uncertainty, especially in the radial and transverse components. The high-frequency modulation is due to the VERITAS orbital period. The improvement during tracking time (represented by gray vertical bands) is seen on the radial component of the position, where the inclusion of tie points allows for a reduction of the uncertainty by nearly 50% uniform through time. Most interestingly, the tie point measurements strongly counteract the buildup of the uncertainty outside the tracking periods, allowing for a more uniform trajectory uncertainty. Indeed, this is because local tie points cover the Doppler tracking gaps. This behavior is clearly visible in Fig. 3, which presents the uncertainty improvement ratio (i.e., the uncertainty ratio between the solutions without and with tie points) during the OD arcs. Figure 3 shows the mean value of the improvement factor (solid line) as well as the 5 and 95% percentiles (shaded area) highlighting the variability across the analyzed OD arcs.

It is worth recalling that radar measurements are not collected during Doppler tracking passes, and the improvement of the performances during tracking time (e.g., a factor 1.5 on radial position and velocity) reflects the better temporal coverage of the motion of the probe during the entire OD arc. Indeed, the better determination of the

trajectory of the probe, empowered by tie points when the spacecraft is not tracked from Earth, allows us to improve the already outstanding tracking system performance, reducing the detrimental propagation effect of loosely resolved position and velocity outside tracking periods. The reduction of the uncertainty buildup outside the tracking periods can be tackled also with standard Doppler tracking analysis techniques, such as the constrained multi-arc analysis (e.g., [22,23]), which constrains the initial position and velocity of the arc $N + 1$ to be equal, within a defined tolerance, to those estimated in arc N . This approach, however, requires the solution of multiple arcs at the same time. The innovation brought by the inclusion of tie points is a strong reduction in the uncertainty buildup phenomenon within a single arc analysis, more suited for real-time processing. The main improvement in terms of positioning is seen on the radial component, which is enhanced by up to a factor of ~ 10 outside of tracking periods. The transverse (along-track) component uncertainty, particularly critical for the horizontal positioning of the radar products, is reduced up to 1.5 outside of tracking passes. Among the velocity components of the probe state vector, the one that benefits the most from tie point measurements is the transversal one, in which a factor of 1.5 gain can be obtained during tracking. This gain increases up to 8 when out of tracking. Figure 3 presents the results also for an increased number of landmarks per orbit showing the dependency of the increase of performances on the number of measured landmarks: the solid, dashed, and dash-dotted lines represent the cases of 10, 20, and 40 landmarks, respectively. As the variability of the results is substantially constant between cases,

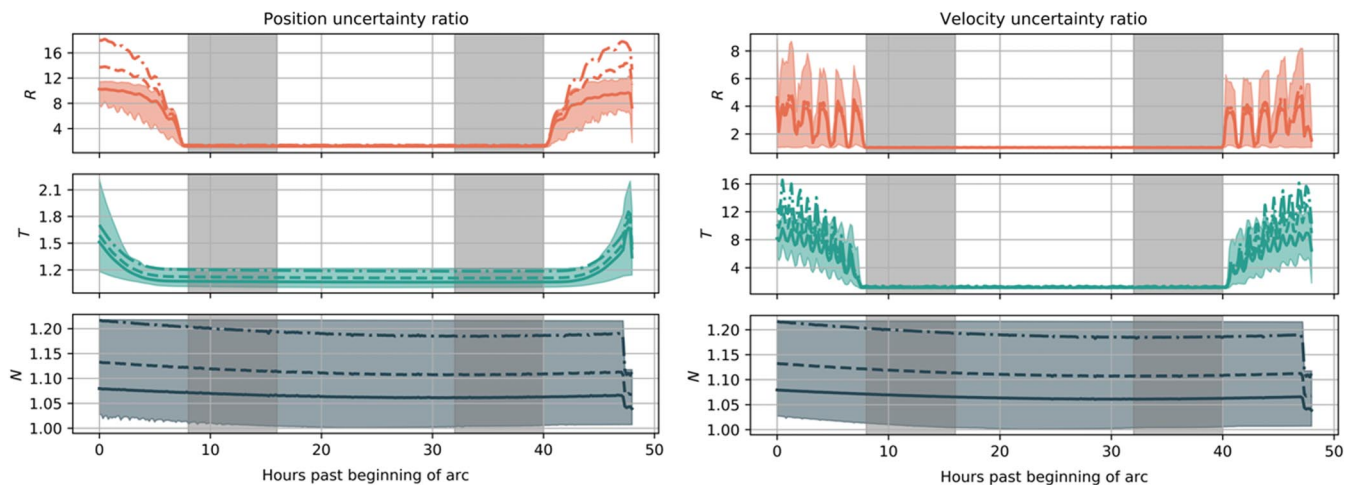


Fig. 3 Uncertainty gain due to the inclusion of different number of tie points (solid line: 10; dashed line: 20; dash-dotted line: 40).

we report the shaded area only for the 10 landmarks case. As expected, a higher number of landmark positions included in the OD process result in a reduction of the state vector components uncertainty (i.e., a larger gain factor).

The results shown until now have been obtained under the assumption of an 8 h update time for the empirical accelerations. The high density of the Venusian atmosphere and its expected complex dynamics (e.g., [24]) may result in a reduction of the required update time of empirical accelerations for capturing higher frequency effects. Augmenting the number of estimated empirical accelerations, however, leads to an inevitable degradation of the orbit reconstruction uncertainty, mainly during out-of-tracking periods. As previously shown, the advantage of using tie points is maximized during these periods, and thus their inclusion can effectively mitigate the detrimental effect of an increased number of empirical accelerations.

We tested this hypothesis by updating the empirical accelerations every 2 h and comparing the results obtained with that of a time update of 8 h. Figure 4 shows the absolute uncertainty results in this case, while Fig. 5 shows the improvement factor as a function of the number of considered landmarks and time. Figure 4 clearly shows the increased buildup of uncertainty in between tracking passes due to the increased number of unknown parameters, related to the empirical accelerations. We observe an increase of a factor ~ 4 in terms of position uncertainty, as compared with the previous case (see Fig. 2). In this case, the relative

tie point contribution is more limited, because of the higher underlying position uncertainty, affecting the landmarks position determination. However, the tie point inclusion still allows a substantial improvement in the trajectory reconstruction capability. It is particularly interesting to assess how in this operational scenario the improvement factor in between tracking passes is improved with respect to the previous case due to the higher instability of the uncertainty propagation entailed by larger number of empirical accelerations. Again, we have repeated the analysis for 10, 20, and 40 landmarks per orbit (solid, dashed, and dash-dotted lines, respectively).

The tie points indeed prove to be helpful in mitigating the detrimental effect of the increased number of empirical accelerations. This is particularly critical for the early phases of the mission when refined models of the gravity field, atmospheric density dynamics, planetary albedo, and other planetary characteristics affecting the trajectory of the probe will not be available yet. In these phases, the number of empirical accelerations included in the OD filter will likely be larger than for the final (end-of-mission) reconstructed orbits when new datasets, produced with global analysis of the entire VERITAS mission, will be available.

The results in Figs. 3 and 5 show a substantial variability among the entire set of 46 analyzed OD arcs, which spans the full range of VERITAS orbit to Earth aspect angle variations. It is then interesting to assess the dependency of the uncertainty reduction factor with

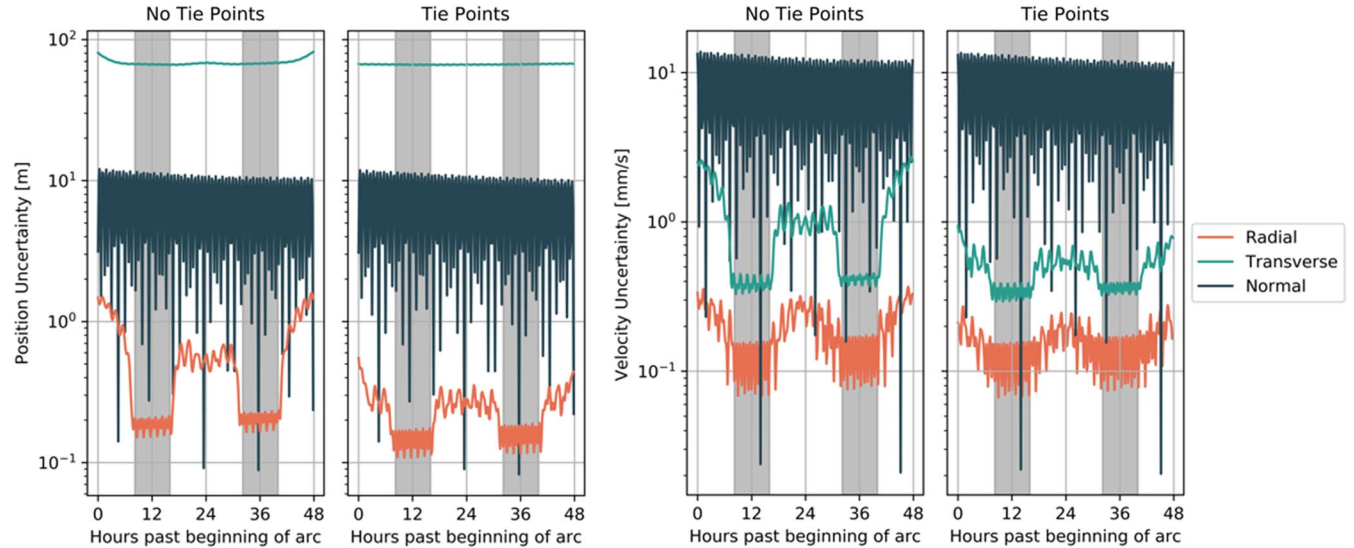


Fig. 4 Position and velocity uncertainty during an OD arc with and without the inclusion of tie points, 2 h empirical acceleration update time (10 per orbit).

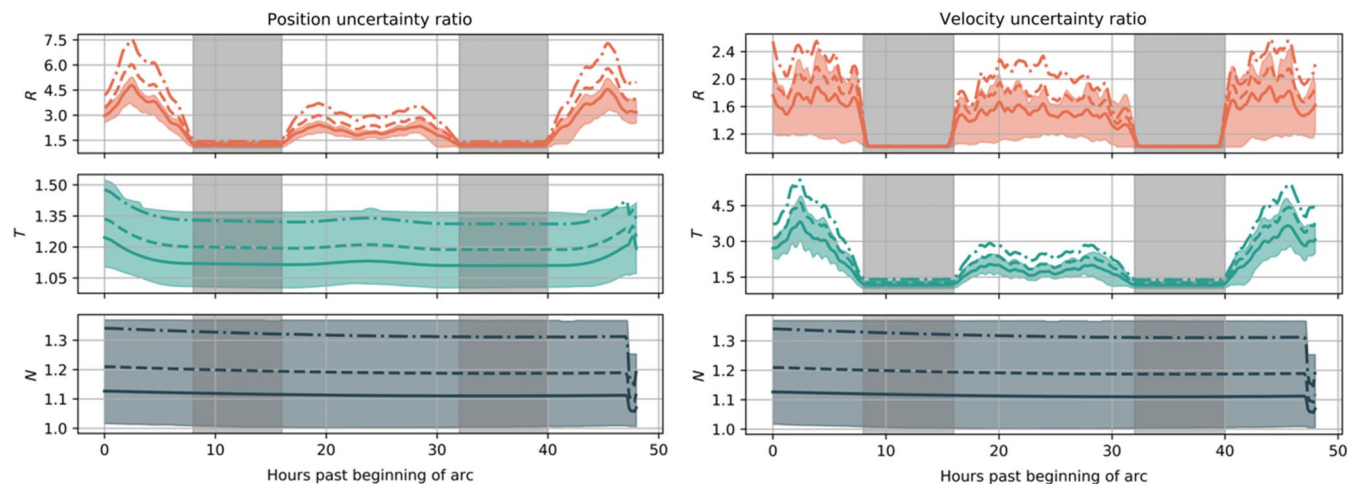


Fig. 5 Uncertainty gain due to the inclusion of different number of tie points, 2 h empirical acceleration update time (solid line: 10; dashed line: 20; dash-dotted line: 40).

respect to the relative geometry between the probe and the Earth. In doing so, we separately analyze the improvement factor attainable before and after the tracking passes (outer) and in between tracking passes (inner), as these two regions show a distinct behavior. Figures 6 and 7 show the improvement factor as a function of the Earth angle α for the inner and outer cases, respectively. We define α as the angle between the VERITAS orbital angular momentum and the Earth direction. It is thus the complement of the Earth β angle discussed in [7]. The 46 OD arcs are chosen to cover the entire range of possible viewing geometries, which includes the extremes of *face on* orbits ($\alpha = 0$) and *edge on* ($\alpha = \pi/2$). Figures 6 and 7 are based on the case with 2-h-update empirical accelerations, as this operational scenario presents more variability in the improvement factor in between tracking passes and thus provides more insight on the variability dependence on the α angle during these periods. All the quantities show a substantial dependence on the α angle with a general trend of increased performances in edge-on orbits, with the exception of the radial position, which shows a nearly constant behavior, and the

transverse velocity component, which shows improved performance when the orbit is nearly face-on or edge-on, while showing smaller improvements at intermediate angles. The general trend of performance variations with the orbital geometry is consistent between the inner and outer cases.

We have, so far, primarily discussed the orbit *reconstruction* capabilities. The process of planning scientific observations, particularly RPI, requires the capability of producing high-quality orbit *predictions*. Figure 8 shows the evolution of the uncertainty reduction gain for a typical OD arc, when the trajectory is propagated two days beyond the last acquired data point. The two quantities that mainly benefit from the inclusion of tie point measurements, namely, radial position and transverse velocity, show a reduction of the gain factor, which stabilizes around ~ 2 . Interestingly, transverse and normal position, radial and normal velocity components show even better performance than during the tracking periods. The qualitative behavior of the absolute uncertainty propagation is identical for the Earth Doppler only and Earth Doppler + tie points cases, but the

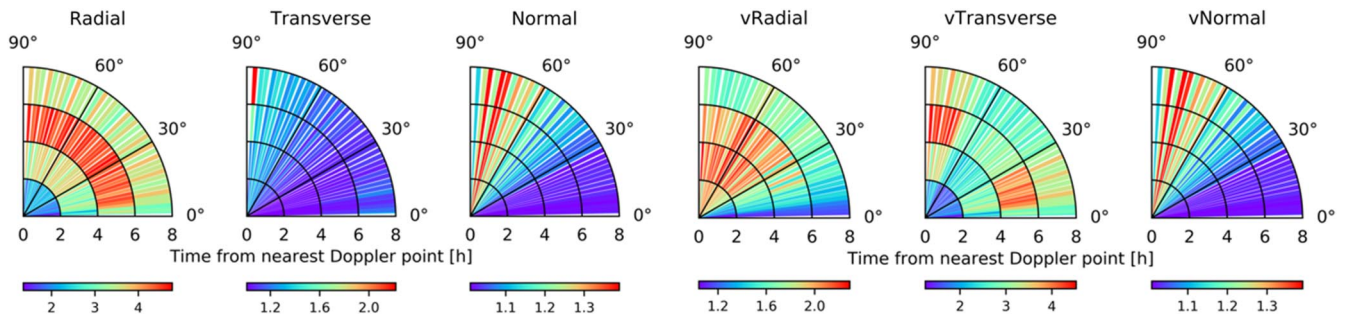


Fig. 6 Uncertainty ratio for position (left) and velocity (right) before and after tracking passes as a function of α (polar angle) and time from the nearest Doppler tracking point.

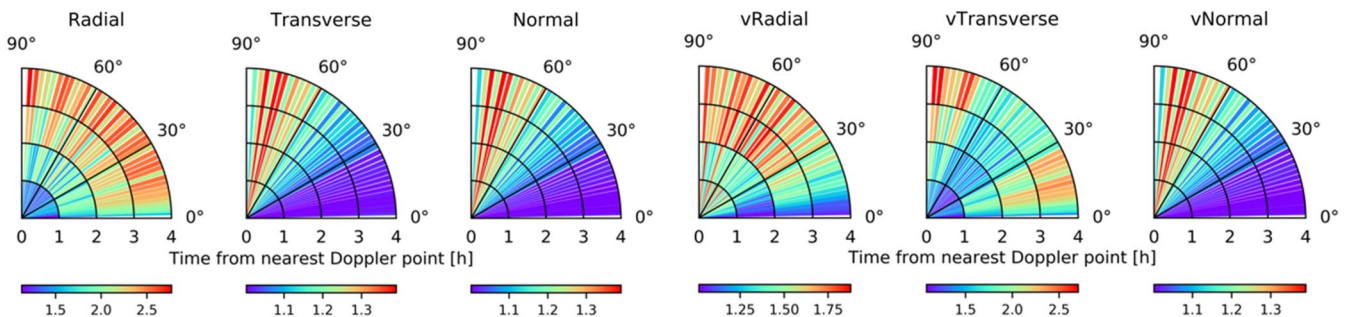


Fig. 7 Uncertainty ratio for position (left) and velocity (right) in between tracking passes as a function of α and time from the nearest Doppler tracking point.

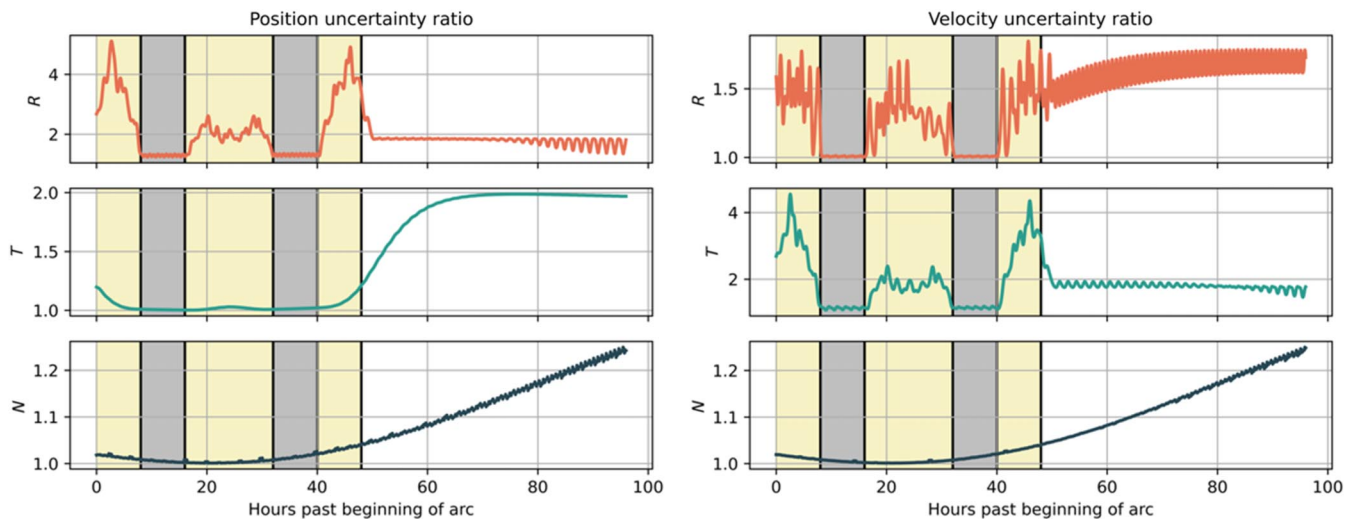


Fig. 8 Uncertainty ratio propagated two days after the nominal end of the OD arc.

characteristic time of the transient from the observation to nonobservation regimes is different. This fact shows in the transient in the uncertainty gain, which tends to asymptotically stabilize around constant values after a first period of fluctuation. The normal position and velocity components (whose asymptotic behavior cannot be seen in Fig. 8) tend to stabilize after ~ 3.5 days around a value of 1.4. The asymptotic stabilization, coupled with the observation of a very similar qualitative behavior of the absolute uncertainty time series, indicates that a general improvement on the prediction uncertainty is due to the generalized uncertainty reduction during the OD arc. The capability of augmenting the predictive performance could prove extremely valuable for scientific observation planning, ultimately contributing to the science return of the mission.

V. Conclusions

The scientific observation targeting and planning capability in the initial phases of planetary orbiter missions strongly relies on the initial trajectory reconstruction and prediction capabilities. In this work, we have shown how the combination of the Earth Doppler tracking and radar tie point datasets could substantially improve VERITAS initial reconstructed orbits. By simulating the nominal mission scenario under different assumptions regarding the number of observed landmarks and dynamic model requirements, we have shown that this combined data analysis strategy can reduce the propagated uncertainty of the probe and thus reduce errors in focused observation targeting and initial scientific product creation and evaluation. The combination of the two datasets could potentially be performed on a routine basis, to provide a uniform improvement in the OD products, or either be requested specifically before critical observation campaigns aiming at high-precision targeting of the instrument on regions of interests on the surface of the planet. Routine use of radar tie-points would require the development of automated processes to identify the landmarks and generate the observables from the radar data. This development is on-going by the VERITAS team at the Jet Propulsion Laboratory. Moreover, non-real-time solutions with tie points can be used to refine the VERITAS dynamic model over time, ultimately providing better observability of nongravitational accelerations and thus a method to cross-check the quality of the Doppler-only solutions. The methods and techniques discussed in this work, although applied to the VERITAS case, are of general nature. The general conclusion of this work can then be applied and extended to other orbital missions with similar instrumentation and observation geometry.

Acknowledgments

Gael Cascioli's work was supported by NASA under award number 80GSFC21M0002. The authors would like to thank the two anonymous reviewers for their valuable comments and suggestions, which helped improving the quality of the paper. Part of this research was carried out at the Jet Propulsion Laboratory, California Institute of Technology, under a contract with the National Aeronautics and Space Administration (80NM0018D0004).

References

- [1] Smrekar, S., Hensley, S., Nybakken, R., Wallace, M. S., Perkovic-Martin, D., You, T.-H., Nunes, D., Brophy, J., Ely, T., Burt, E., Dyar, M. D., Helbert, J., Miller, B., Hartley, J., Kallameyn, P., Whitten, J., Iess, L., Mastrogiuseppe, M., Younis, M., and Mazarico, E., "VERITAS (Venus Emissivity, Radio Science, InSAR, Topography, and Spectroscopy): A Discovery Mission," *2022 IEEE Aerospace Conference (AERO)*, Inst. of Electrical and Electronics Engineers, New York, 2022, pp. 1–20. <https://doi.org/10.1109/AERO53065.2022.9843269>
- [2] Cascioli, G., Hensley, S., de Marchi, F., Breuer, D., Durante, D., Racioppa, P., Iess, L., Mazarico, E., and Smrekar, S. E., "The Determination of the Rotational State and Interior Structure of Venus with VERITAS," *Planetary Science Journal*, Vol. 2, No. 6, 2021, p. 220. <https://doi.org/10.3847/PSJ/ac26c0>
- [3] Mazarico, E., Iess, L., Breuer, D., de Marchi, F., Konopliv, A. S., Hensley, S., and Smrekar, S., "Exploring the Interior of Venus with the VERITAS Gravity Science Investigation," *American Geophysical Union, Fall Meeting 2019, Abstract #P34A-02*, Dec. 2019, <https://ui.adsabs.harvard.edu/abs/2019AGUFM.P34A..02M/abstract>.
- [4] Iess, L., Asmar, S., and Ely, T. A., "Comparison of Different Radio Tracking System Configurations for Planetary Geodesy and Fundamental Physics," *AGU Fall Meeting 2021*, 2021, <https://ui.adsabs.harvard.edu/abs/2021AGUFM.P11D..01I/abstract>.
- [5] Hensley, S., Campbell, B., Perkovic-Martin, D., Wheeler, K., Kiefer, W., and Ghail, R., "VISAR and VenSAR: Two Proposed Radar Investigations of Venus," *2020 IEEE Radar Conference (RadarConf20)*, Inst. of Electrical and Electronics Engineers, New York, 2020, pp. 1–6. <https://doi.org/10.1109/RadarConf2043947.2020.9266323>
- [6] Helbert, J., Säuberlich, T., Dyar, M. D., Ryan, C., Walter, I., Réess, J.-M., Rosas-Ortiz, Y. M., Peter, G., Maturilli, A., and Arnold, G. E., "The Venus Emissivity Mapper (VEM): Advanced Development Status and Performance Evaluation," *Infrared Remote Sensing and Instrumentation XXVIII* edited by M. Strojnik, SPIE, Bellingham, WA, 2020, p. 6. <https://doi.org/10.1117/12.2567634>
- [7] Wallace, M. S., Sweetser, T. H., Haw, R. J., Lau, E., and Hensley, S., "Enabling Repeat-Pass Interferometry from Low Venus Orbit," *Advances in the Astronautical Sciences*, 2019, <https://trs.jpl.nasa.gov/bitstream/handle/2014/49245/CL%2318-7473.pdf?sequence=1>.
- [8] Davies, M. E., Colvin, T. R., Rogers, P. G., Chodas, P. W., Sjogren, W. L., Akim, E. L., Stepanyantz, V. A., Vlasova, Z. P., and Zakharov, A. I., "The Rotation Period, Direction of the North Pole, and Geodetic Control Network of Venus," *Journal of Geophysical Research*, Vol. 97, No. E8, 1992, pp. 13,141–13,151. <https://doi.org/10.1029/92JE01166>
- [9] Chodas, P. W., Wang, T. C., Sjogren, W. L., and Ekelund, J. E., "Magellan Ephemeris Improvement Using Synthetic Aperture Radar Landmark Measurements," *Advances in the Astronautical Sciences*, 1992, <https://ntrs.nasa.gov/citations/19920060678>.
- [10] Chodas, P. W., Lewicki, S. A., Hensley, S., and Masters, W. C., "High Precision Magellan Orbit Determination for Stereo Image Processing," *Advances in the Astronautical Sciences*, 1993, <https://trs.jpl.nasa.gov/handle/2014/35715>.
- [11] Neumann, G. A., Rowlands, D. D., Lemoine, F. G., Smith, D. E., and Zuber, M. T., "Crossover Analysis of Mars Orbiter Laser Altimeter data," *Journal of Geophysical Research: Planets*, Vol. 106, No. E10, 2001, pp. 23,753–23,768. <https://doi.org/10.1029/2000JE001381>
- [12] Mazarico, E., Barker, M. K., Neumann, G. A., Zuber, M. T., and Smith, D. E., "Detection of the Lunar Body Tide by the Lunar Orbiter Laser Altimeter," *Geophysical Research Letters*, Vol. 41, No. 7, 2014, pp. 2282–2288. <https://doi.org/10.1002/2013GL059085>
- [13] Tapley, B. D., Schutz, B. E., and Born, G. H., *Statistical Orbit Determination*, Elsevier, London, 2004, Chap. 3. <https://doi.org/10.1016/B978-0-12-683630-1.X5019-X>
- [14] Cascioli, G., and Genova, A., "Precise Orbit Determination Technique to Refine Spacecraft Mechanical Modeling," *Journal of Spacecraft and Rockets*, Vol. 58, No. 2, 2021, pp. 581–588. <https://doi.org/10.2514/1.A34922>
- [15] Cappuccio, P., Notaro, V., Di Ruscio, A., Iess, L., Genova, A., Durante, D., di Stefano, I., Asmar, S. W., Ciarcia, S., and Simone, L., "Report on First Inflight Data of BepiColombo's Mercury Orbiter Radio Science Experiment," *IEEE Transactions on Aerospace and Electronic Systems*, Vol. 56, No. 6, 2020, pp. 4984–4988. <https://doi.org/10.1109/TAES.2020.3008577>
- [16] Konopliv, A. S., Banerdt, W. B., and Sjogren, W. L., "Venus Gravity: 180th Degree and Order Model," *Icarus*, Vol. 139, No. 1, 1999, pp. 3–18. <https://doi.org/10.1006/icar.1999.6086>
- [17] Justh, H., Justus, C. G., and Keller, V., "Global Reference Atmospheric Models, Including Thermospheres, for Mars, Venus and Earth," *AIAA/AAS Astrodynamics Specialist Conference and Exhibit*, AIAA Paper 2006-6394, 2006. <https://doi.org/10.2514/6.2006-6394>
- [18] Moyer, T. D., "Formulation for Observed and Computed Values of Deep Space Network Data Types for Navigation," *Formulation for Observed and Computed Values of Deep Space Network Data Types for Navigation*, Wiley, Hoboken, NJ, 2003. <https://doi.org/10.1002/0471728470>
- [19] Margot, J.-L., Campbell, D. B., Giorgini, J. D., Jao, J. S., Snedeker, L. G., Ghigo, F. D., and Bonsall, A., "Spin State and Moment of Inertia of Venus," *Nature Astronomy*, Vol. 5, No. 7, 2021, pp. 676–683. <https://doi.org/10.1038/s41550-021-01339-7>

- [20] Pelletier, F., "Cassini Orbit Determination Performance (July 2008–December 2011)," *SpaceOps 2012*, 2012, Paper 1256588, <https://arc.aiaa.org/doi/pdf/10.2514/6.2012-1256588>.
- [21] Evans, S., Taber, W., Drain, T., Smith, J., Wu, H.-C., Guevara, M., Sunseri, R., and Evans, J., "MONTE: the Next Generation of Mission Design and Navigation Software," *CEAS Space Journal*, Vol. 10, No. 1, 2018, pp. 79–86.
<https://doi.org/10.1007/s12567-017-0171-7>
- [22] Alessi, E. M., Cicalò, S., Milani, A., and Tommei, G., "Desaturation Manoeuvres and Precise Orbit Determination for the BepiColombo Mission," *Monthly Notices of the Royal Astronomical Society*, Vol. 423, No. 3, 2012, pp. 2270–2278.
<https://doi.org/10.1111/j.1365-2966.2012.21035.x>
- [23] Iess, L., Asmar, S. W., Cappuccio, P., Cascioli, G., de Marchi, F., di Stefano, I., Genova, A., Ashby, N., Barriot, J. P., Bender, P., Benedetto, C., Border, J. S., Budnik, F., Ciarcia, S., Damour, T., Dehant, V., di Achille, G., di Ruscio, A., Fienga, A., and Zannoni, M., "Gravity, Geodesy and Fundamental Physics with BepiColombo's MORE Investigation," *Space Science Reviews*, Vol. 217, No. 1, 2021.
<https://doi.org/10.1007/s11214-021-00800-3>
- [24] Müller-Wodarg, I. C. F., Bruinsma, S., Marty, J.-C., and Svedhem, H., "In Situ Observations of Waves in Venus's Polar Lower Thermosphere with Venus Express Aerobraking," *Nature Physics*, Vol. 12, No. 8, 2016, pp. 767–771.
<https://doi.org/10.1038/nphys3733>
- [25] Konopliv, A. S., and Yoder, C. F., "Venusian k_2 Tidal Love number from Magellan and PVO Tracking Data," *Geophysical Research Letters*, Vol. 23, No. 14, 1996, pp. 1857–1860.
<https://doi.org/10.1029/96GL01589>

C. W. Roscoe
Associate Editor